J. Fluid Mech. (1974), *vol.* 63, *part* 2, *pp.* 301–314
Printed in Great Britain

The spectral evolution of sedimentary bed forms

By SUBHASH C. JAIN AND JOHN F. KENNEDY
Institute of Hydraulic Research, The University of Iowa, Iowa City

(Received 1 March 1973 and in revised form 14 August 1973)

A potential-flow based analytical model is developed for the temporal development of the spectra of ripples and dunes generated on an initially flattened bed by an open-channel flow. The analysis predicts the occurrence of two distinct spectral peaks at small times; the physical origin of each is explained. One of the peaks has spatial frequency equal to that given by the Airy relation for a small amplitude stationary free-surface wave. These results are confirmed by Jain's (1971) experimental data. Jain's data also are used to determine quantitative values of the lag distance and Hayashi's (1970) inclination factor, α, which appear in the sediment-transport relation used in the analysis. A variance-cascade model is used to derive the 'minus-three-power law' that describes the spatial spectra of ripples and dunes at higher wavenumbers. Finally, the relation between the Froude number and dominant wavelength implied by Jain & Kennedy's (1971) non-dimensionalized spectra is discussed and compared with data presented by Jain (1971) and Nordin (1971).

1. Introduction

An initially flat bed composed of non-cohesive sedimentary material and bounding a turbulent flow will remain flat only over limited ranges of flow depth and velocity; at Froude numbers less than about 0·5–0·7 the bed surface generally will be deformed into the migrating waves known as ripples or dunes, while at larger Froude numbers antidunes may be generated.† The principal characteristics of developing sand ripples generated by open-channel flows have been described by Raichlen & Kennedy (1965) and Jain & Kennedy (1971), and may be summarized as follows. The first waves formed on a plane bed are primarily two-dimensional, with continuous crests and troughs that are much longer than the wavelength, and are very uniform in shape and spacing. As the ripples grow and mature, their wavelength increases rapidly and their two-dimensionality and geometrical regularity soon degenerate as the bed forms become short-crested and markedly three-dimensional. Fully developed ripples and dunes are so irregular geometrically that it is difficult to describe them quantitatively in other than statistical terms. This evolution of ripples from regular two-dimensional waves to a somewhat erratic pattern of peaks and pockets is illustrated in the sequential photographs obtained by Jain & Kennedy (1971) in the course of laboratory flume experiments on bed-form evolution.

† A.S.C.E. Task Force on Bed Forms in Alluvial Channels, 1966: 'Nomenclature for bed forms in alluvial channels'. *Proc. A.S.C.E., J. Hyd. Div.* **92**, 51–64.

So far two principal lines of inquiry have been pursued in attempts to describe and formulate the mechanisms responsible for the occurrence of sedimentary bed forms. In the first type of analysis, the kinematics and dynamics of the liquid and solid phases and of the interaction between the flow and the bed during the early stages of formation have been formulated and examined to ascertain the conditions for occurrence and the geometrical and kinematical properties of the various bed forms. The theoretical models presented by Anderson (1953), Kennedy (1963, 1969), Reynolds (1965), Gradowczyk (1968, 1971), Smith (1970) and Engelund (1970) fall into this category. The second approach has involved use of statistical descriptors, principally the spectral density function, of sedimentary bed forms and has sought to adduce therefrom information concerning the mechanics of growth, migration and maintenance of the bed profiles. This avenue of investigation was introduced by Nordin & Algert (1966), and has been pursued by Ashida & Tanaka (1967), Nordin (1971), Engelund (1969) and Jain & Kennedy (1971). Hino (1968) presented an analysis based on dimensional arguments to explain the 'minus-three-power law' that characterizes the spatial spectra of ripple and dune profiles at higher wavenumbers.

In the present paper an attempt is made to combine aspects of both of the lines of investigation described above. A relation is derived for the evolution with time of the spectra of ripples and dunes, and a new derivation based on a variance-cascade process is presented for the minus-three-power property of the high frequency segment of bed-form spectra.

2. Potential-flow model for the initial evolution of ripple and dune spectra

Consider the two-dimensional, irrotational, free-surface flow of an incompressible fluid over an erodible bed. Let d be the mean depth of the flow over the wavy bed and U be the velocity in the positive x direction of the primary flow, as shown in figure 1. The origin of the vertical y co-ordinate, positive upward, is taken at the undisturbed free surface. Let the free-surface and bed profiles be given by $y = \xi(x,t)$ and $y = -d+\eta(x,t)$, respectively. The amplitudes of ξ and η are assumed to be small compared with the wavelength of the bed features and the flow depth. The linearized boundary conditions on the upper and lower boundaries are

$$\left.\begin{aligned} \xi_t + U\xi_x &= \phi_y \\ g\xi + U\phi_x + \phi_t &= 0 \end{aligned}\right\} \quad \text{on} \quad y = 0, \tag{1, 2}$$

$$\eta_t + U\eta_x = \phi_y \quad \text{on} \quad y = -d, \tag{3}$$

where the subscripts x, y and t indicate partial differentiation with respect to space and time co-ordinates, and ϕ is the harmonic velocity potential whose gradient is the velocity field due to just the waviness of the bed.

The streamwise profile of the bed will be described as a stationary random process. Thus let $\eta(x,t)$ be expressed in terms of its Fourier transform as

$$\eta(x,t) = \int B(k,t)\, e^{ikx}\, dx, \tag{4}$$

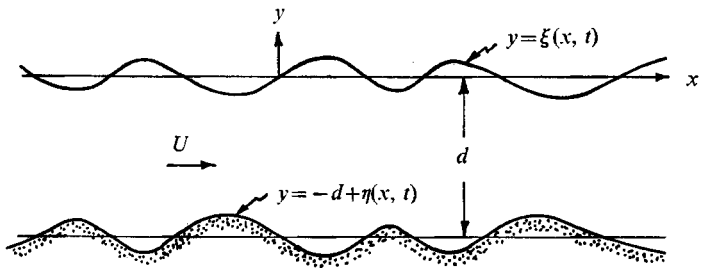

FIGURE 1. Definition sketch of free-surface flow over an irregular erodible bed.

where $k = 2\pi/L$ is the wave number. The harmonic potential function, expressed as a generalized Fourier transform, which fulfils the boundary conditions (1)–(3), is

$$\phi(x,y,t) = iU\int JB(k,t)\,e^{ikx}\,dx, \tag{5}$$

where

$$J(k,y) = \frac{\cosh ky + F^2kd\sinh ky}{F^2kd\cosh kd - \sinh kd}, \tag{6}$$

in which $F^2 = U^2/gd$. In deriving (5), B_t has been assumed to be small compared with BUk. The continuity equation for the sediment phase of the motion, relating the time rate of change of the local bed elevation and the streamwise variation of the local sediment-transport rate, is

$$\eta_t + T_x = 0, \tag{7}$$

in which T is the local volume rate of sediment transport per unit width. To close the formulation it is necessary to have an additional relation between T and η or ϕ; this is the sediment-transport relation. The transport relation adopted here is a slightly modified form of the one proposed by Hayashi (1970):

$$T(x,t) = m[1+\alpha\eta_x(x,t)]\,[(U-U_c)+\phi_x(x-\beta,-d,t)]^n, \tag{8}$$

in which m is a dimensional coefficient, α and n are dimensionless constants, β is the distance by which the local sediment-transport rate lags behind the local velocity at the mean level of the bed, and U_c is the critical velocity which just initiates particle movement. Substitution of (8) into (7) yields, since $|\phi_x/(U-U_c)| \ll 1$,

$$\eta_t(x,t) + \overline{T}[\alpha\eta_{xx}(x,t) + n(U-U_c)^{-1}\phi_{xx}(x-\beta,-d,t) + O(\phi_2^x)] = 0, \tag{9}$$

in which $\overline{T} = m(U-U_c)^n$ is the average rate of sediment transport along the bed at any time.

Taking the generalized Fourier transform of (9) and substituting for ϕ from (5) gives

$$B_t(k,t) - \overline{T}k^2[\alpha - in_1J_1\exp(-ik\beta)]\,B(k,t) = 0, \tag{10}$$

in which

$$J_1 = -J(k,-d) = \frac{\cosh kd - F^2kd\sinh kd}{\sinh kd - F^2kd\cosh kd}$$

and

$$n_1 = nU/(U-U_c).$$

The solution of (10) is

$$B(k,t) = B(k,0)\exp[\overline{T}k^2\{\alpha - in_1J_1\exp(-ik\beta)\}t]. \tag{11}$$

Forming the product of $B(k,t)$ with its complex conjugate $B^*(k,t)$ gives

$$\overline{B(k,t)\,B^*(k',t)} = \overline{B(k,0)\,B^*(k',0)}\exp[\overline{T}k^2\{\alpha - in_1 J_1 \exp(-ik\beta)\}t] \times \exp[\overline{T}k'^2\{\alpha + in_1 J_1' \exp(ik\beta)\}t], \quad (12)$$

where $J_1' = -J(k', -d)$ and an overbar denotes an ensemble average. Introduction of the relation

$$\Phi(k,t)\,\delta(k-k') = \overline{B(k,t)\,B^*(k',t)},$$

where Φ is the spectrum of the bed elevation and δ is the Dirac delta-function, into (12) and integration over all positive k' yield

$$\Phi(k,t) = \Phi(k,0)\exp[2\overline{T}k^2(\alpha - n_1 J_1 \sin k\beta)t]. \quad (13)$$

The speed c of the contribution to Φ with wavenumber k is found from (4) and (11) to be

$$c = \overline{T}n_1 k J_1 \cos k\beta. \quad (14)$$

The dependence of c on k indicates that the bed waves are dispersive.

Over those ranges of k for which $\alpha - n_1 J_1(kd, F^2)\sin k\beta$, appearing in (13), is positive, Φ increases with time as $\exp(2t)$; accordingly, the bed is expected to be unstable with respect to disturbances having those frequencies, with the resultant generation of bed waves. Furthermore, one might expect that the dominant wavelength that occurs at small times is that for which the initial growth rate of the spectral density function is maximum. From (13), the initial normalized rate of amplification is

$$\frac{\Phi_t(k,0)}{\Phi(k,0)}\frac{d^2}{2T\alpha} = k^2d^2\left(1 - \frac{n_1}{\alpha}J_1 \sin k\beta\right) \equiv \Gamma. \quad (15)$$

The variation of Γ with kd for $n_1/\alpha = 1{\cdot}0$, $\beta/d = 0{\cdot}72$ and $F = 0{\cdot}44$ is shown in figure 2. Equation (15) is seen to have a singularity at the Airy speed; i.e. at

$$F^2 = \tanh kd/kd. \quad (16)$$

It is this singularity, which occurs at the wavelength for which the speed of a small amplitude surface wave in a flow with depth d is just equal to the mean flow speed, that is responsible for the spike extending to $\pm\infty$ in figure 2. The bed–flow interaction for this 'resonant' case can be analysed, at least approximately, as follows. The velocity potential ϕ_1 for the wave-induced velocities of stationary surface waves of wavelength L on a flow with depth d and mean velocity U over a plane bed is

$$\phi_1 = UA\frac{\cosh k(y+d)}{\sinh kd}\cos kx, \quad (17)$$

where A is the surface-wave amplitude. Substituting ϕ_1 from (17) for ϕ in (9), noting that $\eta_x = 0$ for the initially plane bed, and carrying out one integration leads to

$$\eta = \left[n\overline{T}\frac{U}{(U-U_c)}\frac{Ak^2}{\sinh kd}\cos k(x-\beta)\right]t, \quad (18)$$

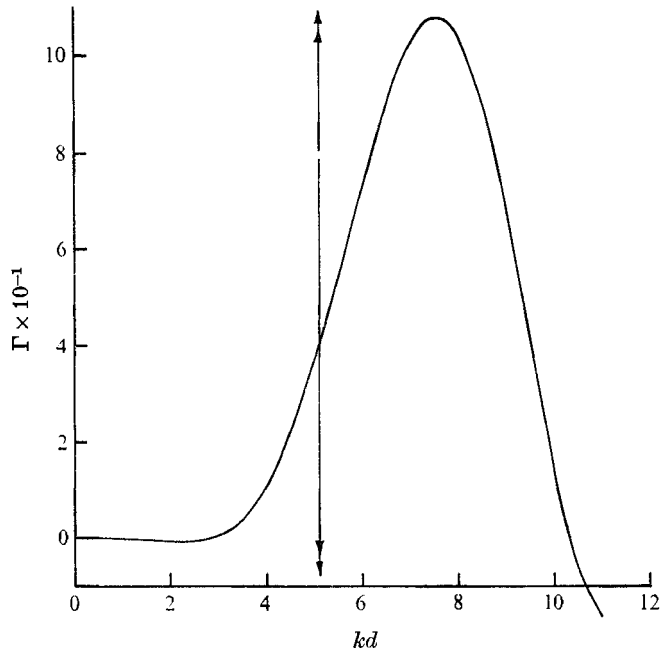

FIGURE 2. Variation of normalized growth rate Γ with kd, calculated from (15) for $\eta_1/\alpha = 1{\cdot}0$, $\beta/d = 0{\cdot}72$ and $F = 0{\cdot}44$.

with U and kd related by the Airy formula, (16). Equation (18) demonstrates the initial linear growth with time on even an absolutely flat erodible boundary of a bed wave with wavelength given by (16).

3. The occurrence of spectral peaks

Figure 3, in which $\bar{\Phi}$ is the spectral estimate calculated from the measured bed profiles, presents a typical set of spectra measured by Jain (1971). In his experiments the bed was initially flattened over the full 90 ft length of the 3 ft wide laboratory flume he used, and longitudinal bed profiles were measured, with a sonic probe mounted on a motorized carriage, at short time intervals after the flow was started until the bed reached its equilibrium configuration. In all experiments (with the exception of one, his run S-3, for which the bed configuration was in the transition state between the ripple and flat bed regimes) he found that the spectra measured at small times are characterized by two distinct peaks; e.g. those at kd values of about 4 and 8 in figure 3. This is precisely the behaviour predicted by (13) and (15) and illustrated in figure 2. In fact, the values of β/d and n_1/α adopted for figure 2 were selected to fulfil two requirements relative to the spectra in figure 3: that the second peak (that at the higher spatial frequency) of Γ given by (15) and that of the spectrum measured at the smallest time ($t = 3$ min) occur at the same value of kd; and that the first frequency beyond the second peak at which $\Gamma = 0$ be that for which the spectrum measured at small times is equal to 5% of its value at the high-frequency peak. This procedure

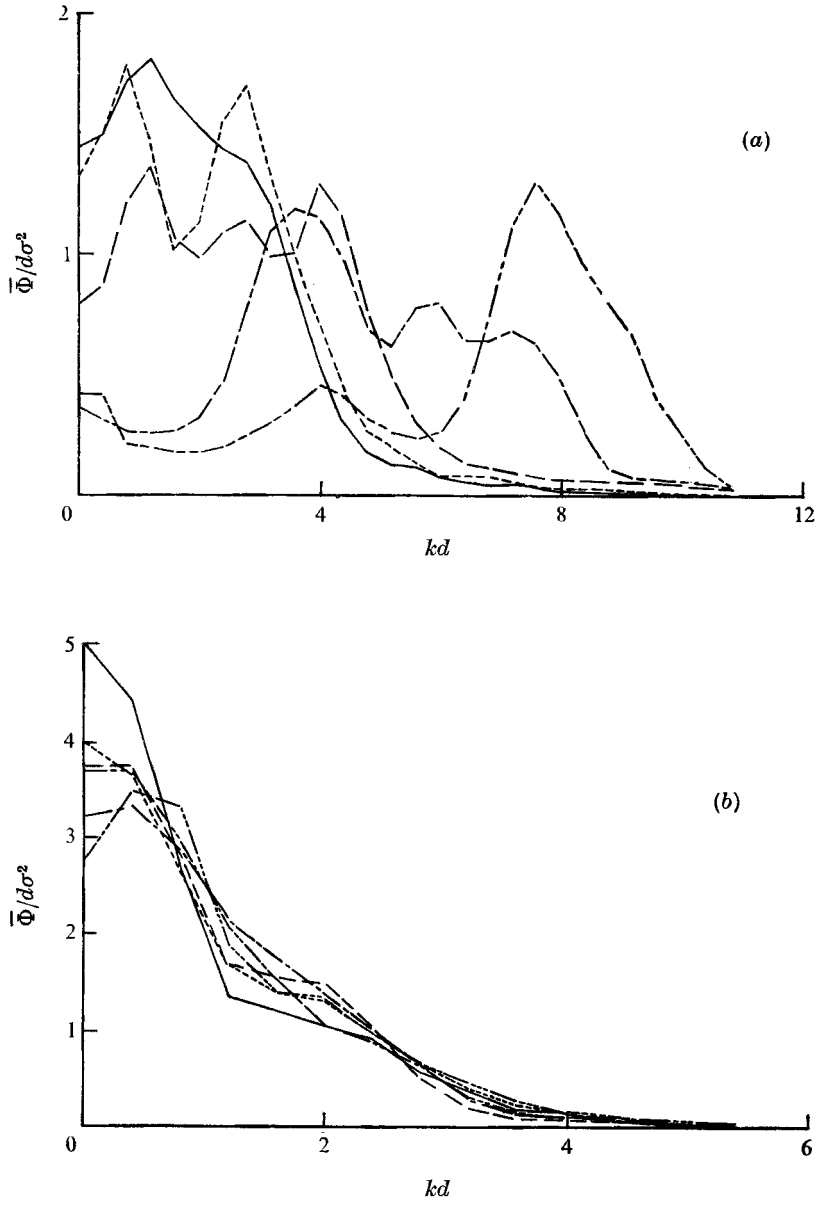

FIGURE 3. Spectra of evolving bed profiles measured at successive times in a laboratory flume experiment (Jain 1971, run S-8). (*a*) t (min): ——, 3; — · —, 6; – – –, 12; - - - - -, 18; ——, 24. (*b*) t (min): — · · · —, 42; — · · —, 54; — · —, 78; – – –, 108; - - - - - -, 156; ——, ∞.

Run	Depth d (ft)	Mean Velocity U (ft/s)	Froude number F	Water temperature T (°C)	Slope $\times 10^4$ S	Shear velocity u_* (ft/s)	Friction factor f	Sediment discharge $\times 10^5$ $\bar{T}$ (ft²/s)	Bed condition	n_1/α	n/α ($U_c = 0{\cdot}8$ ft/s)	β/d	β (ft)
S-1	0·36	1·21	0·37	28·5	15·4	0·12	0·074	1·01	Ripples	1·42	0·48	0·53	0·19
S-2	0·33	1·62	0·50	20·0	19·3	0·13	0·051	15·1	Ripples	1·04	0·53	0·61	0·20
S-3†	0·32	1·92	0·60	21·8	16·5	0·12	0·030	$\frac{24{\cdot}1}{76{\cdot}3}$	Transition	1·12	0·65	0·72	0·23
S-4	0·35	1·32	0·39	25·5	16·3	0·12	0·070	3·40	Ripples	1·00	0·40	0·54	0·19
S-5‡	0·33	1·41	0·43	21·0	18·4	0·13	0·065	8·42	Ripples	—	—	0·58	0·19
S-6	0·27	1·33	0·45	21·0	25·4	0·14	0·083	4·15	Ripples	1·18	0·47	0·68	0·18
S-7	0·25	1·44	0·51	21·0	25·6	0·13	0·068	6·95	Ripples	1·15	0·51	0·80	0·20
S-8	0·25	1·26	0·44	21·0	26·7	0·14	0·094	3·75	Ripples	1·00	0·37	0·72	0·18
S-9	0·25	1·14	0·40	24·0	25·6	0·13	0·110	2·99	Ripples	1·03	0·31	0·73	0·18
S-10	0·40	1·56	0·43	24·0	14·6	0·12	0·050	9·51	Ripples	1·92	0·94	0·41	0·17
S-11	0·44	1·35	0·36	26·0	12·2	0·12	0·059	2·16	Ripples	1·22	0·50	0·39	0·17
S-12§	0·42	1·11	0·30	25·0	10·9	0·11	0·074	1·16	Ripples	2·65	0·74	0·61	0·25

† Bed configuration in transition regime. Spectra computed only for ripple-covered reaches of bed.

‡ No spectral data for $t = 3$ min. α could not be determined from spectra at larger t.

§ Evolution of bed configuration very slow, due to low transport rate. First bed profile measured at $t = 24$ min.

TABLE 1. Summary of data from Jain's (1971) experiments. Mean sand diameter = 0·25 mm. Sand geometric standard deviation = 1·4. Flume width = 3·00 ft.

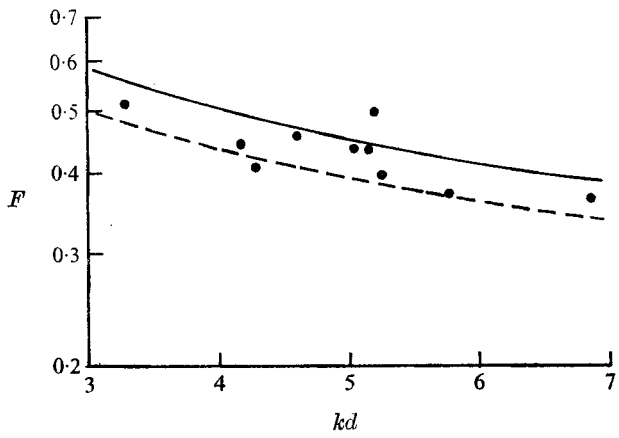

FIGURE 4. Comparison of theoretical and observed (Jain & Kennedy 1971) values of kd at the first spectral peak. ——, equation (16); - - - -, Lighthill's (1953) modified wave-speed relation.

was used to determine the values of β/d and n_1/α for all of the experiments reported by Jain (1971); the results are summarized in table 1, together with other relevant data from his experiments. In the course of the data analysis, it was found that for a given set of flow conditions β is dependent primarily on the value of kd at which the second spectral peak occurs. The estimate of n_1/α, on the other hand, is influenced strongly by the value of $\overline{\Phi}$ and corresponding kd selected as the cut-off value ($\overline{\Phi} = 5\,\%$ of its value at the second peak, in the present analysis). It is seen in table 1 that β is nearly constant for the limited range of conditions investigated in this study. The quantity n_1/α also appears not to vary too widely; however, the estimates obtained for it are much less reliable than those of β/d, for the reason just noted.

The first spectral peak (that at the lower value of kd) appearing at small times in figure 3 corresponds to the singularity in (13) and (15) that arises at the Airy speed given by (16). Figure 4 presents a comparison of the measured values of kd at which the first spectral peaks were observed in Jain's (1971) experiments to occur at small times, the Airy relation, and the wave celerity relation modified by Lighthill (1953) for the $\frac{1}{7}$-power-law velocity distribution to take account of the effect of the vorticity in a turbulent open-channel flow. The correspondence between the observed and expected values of kd is seen to be quite satisfactory.

The principal conclusions to be reached at this point from the foregoing analysis and Jain's (1971) experimental results may be summarized as follows. At small times the spectra of bed forms developing on an initially flat bed are characterized by two peaks. One peak, generally that at the lower spatial frequency, traces its origin to the velocity-field perturbation and accompanying pattern of differential deposition and scour on the bed produced by a small amplitude, stationary surface wave; i.e. a wave train moving relative to the fluid with velocity just equal in magnitude but opposite in direction to the mean flow velocity. It is this equality that determines the frequency of one spectral peak. The second peak

corresponds to bed waves resulting from the inherent instability of an interface between an erodible bed and a turbulent flow. Over wide ranges of flow conditions any small initial disturbance on an otherwise flat bed will produce a perturbation of the velocity field and hence also of the sediment-transport distribution, giving rise to a spatial pattern of scour and deposition that produces bed waves. This instability mechanism is not dependent on the proximity of a free surface; it also produces, for example, ripples in very deep tidal flows and aeolian ripples on wind-swept sand deposits. The spatial frequency at which it is centred is a function of the flow and transport characteristics, reflected in n_1/α, J_1 and β/d, and can be expected to occur at the value of kd where Γ, given by (15) and illustrated in figure 2, has a continuous maximum. Equation (14) indicates that the two different families of waves will move with different speeds, and this frequency dispersion probably accounts for the shift of the normalized spectra, apparent in figure 3, towards the lower frequencies as the bed configurations develop and mature; this notion is explored in the next section.

4. Evolution of the spectra to equilibrium

The shift of the normalized spectra towards progressively lower frequencies as the bed configuration matures, noted above, is such a striking and general feature of the spectra reported by Jain (1971) that it deserves elucidation. A possible explanation is as follows. The two mechanisms described above produce two initial spectral peaks, each with a different dominant wavenumber. Equation (14) demonstrates that the waves with larger k will move faster than those with lower values; hence the shorter waves will overtake the longer, slower-moving ones. However, sedimentary waves cannot pass through each other, as can deformation waves in a continuous medium, and therefore the shorter waves will be absorbed by the longer, slower-moving ones to form new waves which will be longer and higher than the two waves which merged, and which will move still more slowly. In this merger, bed-wave variance generated at higher frequencies will be shifted to a lower frequency. This process will continue until the bed waves become so high that they reach a limiting steepness and cannot grow further, or so long that they are attenuated by the flow over those ranges of k where Γ is negative [see (15) and figure 2]. Thus one can envisage a situation in which bed waves are continuously generated at larger wavenumbers, by the mechanisms described above, and overtake one another and merge into progressively longer and higher waves until the wavelength and amplitude become so great that the bed-wave variance is attenuated at lower wavenumbers by the flow at the same rate as that at which it is generated by the instability mechanisms at higher wavenumbers and transported into the lower wavenumbers. The model outlined above also provides a possible explanation for wind-generated ripples generally being nearly monochromatic while those generated by flowing water exhibit a wide range of wavelengths. In the case of the aeolian bed forms, there is no free surface present to interact with the bed and generate a second spectral peak. Hence there is not a wide range of different frequencies generated, which interact and produce yet other frequencies.

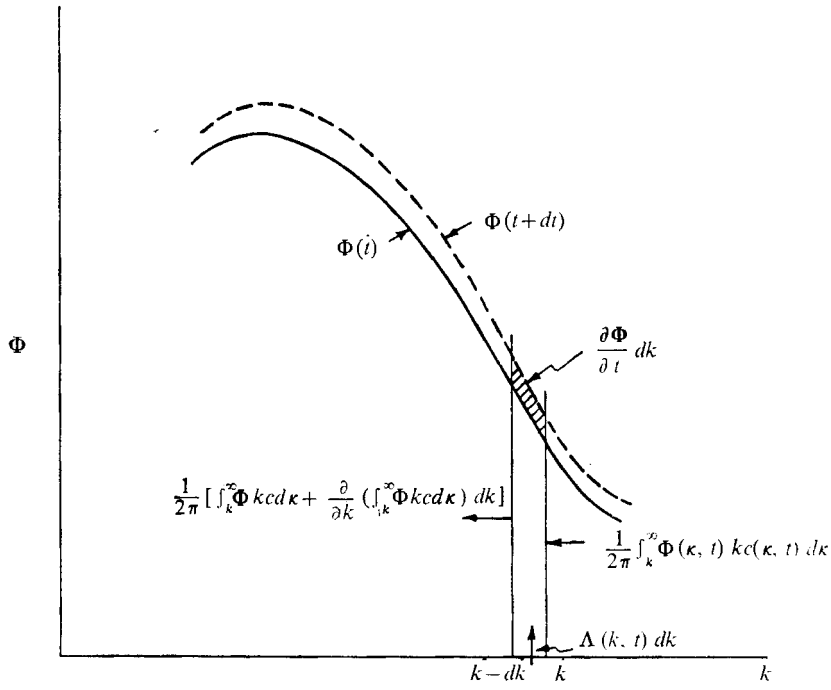

FIGURE 5. Schematic representation of differential relation for bed-wave variance, equation (19).

The variance cascade described above may be formulated on the basis of a variance-conservation concept, as follows. The time rate of change of the contribution to the total variance contained between wavenumbers k and $k-dk$ equals the rate of variance production between k and $k-dk$, plus the difference between the variance flux through k and $k-dk$. This continuity relation is depicted schematically in figure 5 and is expressed mathematically as

$$\frac{\partial}{\partial t}\Phi(k,t)\,dk = \Lambda(k,t)\,dk + \frac{1}{2\pi}\left\{\int_k^\infty \Phi(\kappa,t)\,kc(\kappa,t)\,d\kappa - \left[\int_k^\infty \Phi(\kappa,t)\,kc(\kappa,t)\,d\kappa - \frac{\partial}{\partial k}\left(\int_k^\infty \Phi(\kappa,t)\,kc(\kappa,t)\,d\kappa\right)dk\right]\right\}, \qquad (19)$$

in which $\Lambda(k,t)$ is the rate of variance production at wavenumber k, and the characteristic time required for a wave with wavenumber κ to merge with one of number k is assumed to be proportional to $[kc(\kappa,t)/2\pi]^{-1}$. At this stage it is not possible to solve (19) because of the many uncertainties surrounding the various terms it contains. However, an important conclusion can be derived for fully developed bed profiles. Let it be assumed that there exists a certain range of wavenumbers $k_0 < k < k_1$ over which there is neither production nor dissipation of variance; i.e. over which Λ is zero. For these wavenumbers and steady-state conditions, (19) reduces to

$$\frac{d}{dk}\left(k\int_k^\infty \Phi c\,d\kappa\right) = 0. \qquad (20)$$

For sufficiently large kd, J_1 approaches unity and (14) becomes

$$c \simeq \bar{T}\eta k \tag{21}$$

if, as concluded by Kennedy (1969), $\cos k\beta \sim 1$ for equilibrium bed profiles. Introducing (21) into (20) and solving for Φ yields

$$\Phi \sim k^{-3}. \tag{22}$$

This power law for sediment waves has been derived by Hino (1968) on the basis of dimensional considerations. Kolmogorov's '$-\frac{5}{3}$-power law' for the inertial subrange of turbulent velocity fluctuations also has been derived (Jain 1971) from an approach parallel to that used above.

Figure 6 presents the spectral data reported by Jain (1971) plotted in the non-dimensional format proposed by Jain & Kennedy (1971). It is seen that the data conform nicely to (22) for $dF^{\frac{5}{3}}/L$ greater than about 10^{-1}. For the normalizing parameters used in figure 6, the wavelength L_2, defined as

$$L_2 = (M_0/M_2)^{\frac{1}{2}}, \tag{23}$$

where

$$M_r = \int_0^\infty \bar{\Phi} \left(\frac{1}{L}\right)^r d\left(\frac{1}{L}\right), \tag{24}$$

is given by

$$L_2/d \sim F^{\frac{5}{3}}. \tag{25}$$

Kennedy's (1969) analysis yields

$$L_m/d \sim F^2 \tag{26}$$

for the expected wavelength L_m of monochromatic waves at higher frequencies. Figure 7, which is based on Jain's (1971) and Nordin's (1971) data,† indicates that the analytical result given by (26) would conform better with Jain's (1971) experimental data on L_2 determined from spatial spectra if the exponent were $\frac{5}{3}$, while Nordin's results, on the other hand, are in satisfactory agreement with (26). It was found that the experimental spectral data presented non-dimensionally in figure 6, as well as those of Nordin (1971) and of Ashida & Tanaka (1957), are all grouped more tightly about a single curve if $F^{\frac{5}{3}}$ instead of F^2 is used in the normalizing factors.

5. Concluding remarks

The relation developed for the evolution of bed-form spectra, equation (13), does not predict the shift of the spectra toward lower frequencies as the bed configurations mature. This is because the analysis leading to (13) did not incorporate any information about shorter waves overtaking and being captured by the longer ones. When this feature, described and formulated in § 4, is incorporated into the formulation developed in § 2, the analysis becomes quite complex. This would appear, however, to be the next logical step in the analysis of sand-wave spectra.

† The analysis of Nordin's data included only those experiments for which the spectra were reported.

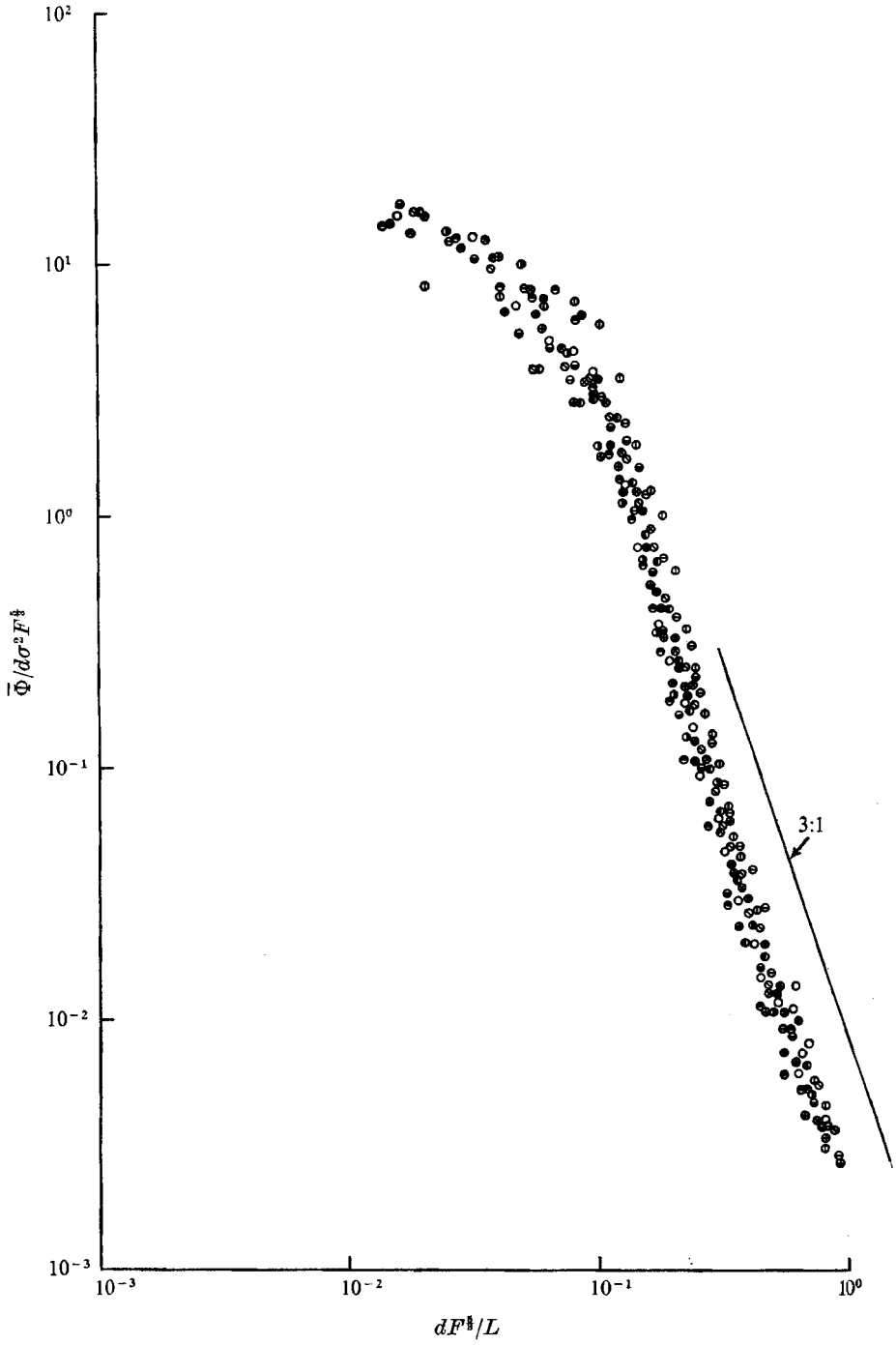

FIGURE 6. Non-dimensional plot of Jain's (1971) spectra data illustrating occurrence of minus-three-power law at higher frequencies.

	⊕	⊖	◓	◒	⊗	⊕	◐	◑	○	⊘	●
U (ft/s)	1·410	1·625	1·145	1·262	1·330	1·442	1·350	1·560	1·210	1·320	1·110
d (ft)	0·329	0·331	0·248	0·253	0·267	0·246	0·437	0·402	0·335	0·353	0·417

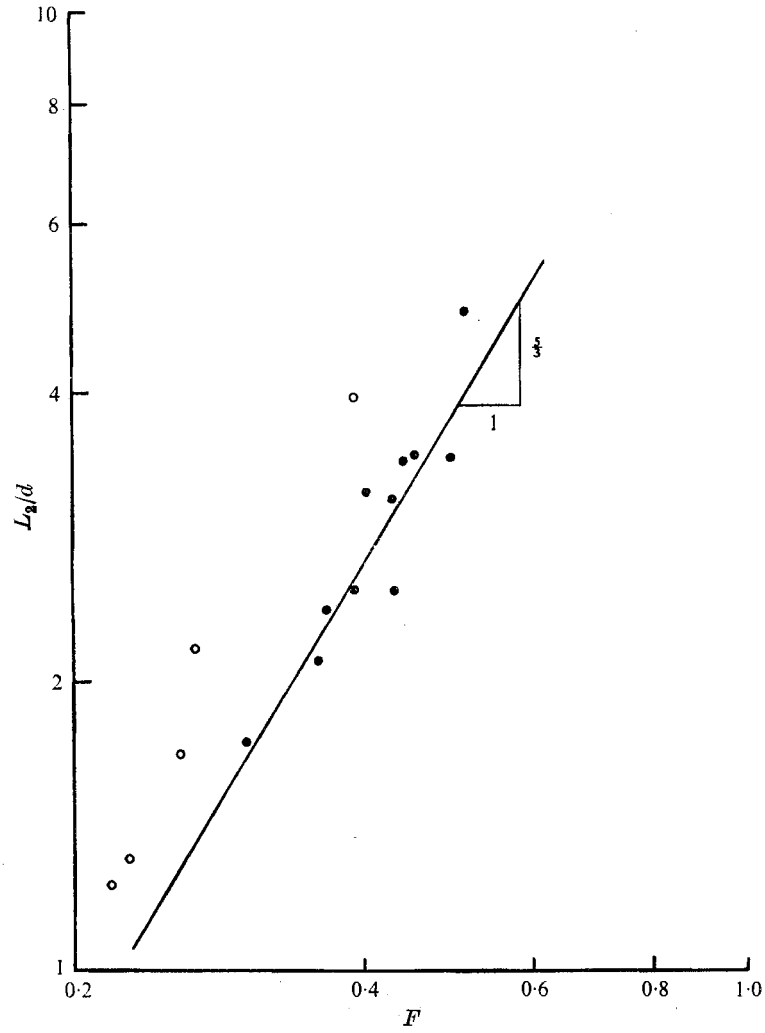

FIGURE 7. Relation between F and normalized wavelength for Jain's (1971) and Nordin's (1971) data. ●, Jain's data; ○, Nordin's data.

The sediment-transport parameters α and β were introduced in (8) and evaluated from the spectra measured by Jain (1971). One could, no doubt, adopt other forms of transport relations and obtain analytical results that also are in satisfactory agreement with experimental data. The free parameters which the alternative formulations would contain could very likely also be evaluated from the spectra of developing bed forms. The point is that the understanding and formulation of the local sediment-transport rate in non-uniform flow at present are so imperfect that one is compelled to incorporate into analytical models of the mechanics of sedimentary bed forms rather primitive relations for the local sediment discharge. These relations will almost invariably contain one or more undetermined coefficients. The method proposed here for evaluating n_1/α and β provides a technique for determination of those coefficients. One

should keep in mind, however, that their values are likely to change as the bed forms develop and may be quite different for equilibrium conditions. Perhaps they can best be determined then from data on the dominant wavelength and wave speed of fully developed bed forms.

Jain's experiments and the analysis presented in §§ 2 and 4 were carried out in a research programme sponsored by the Iowa State Water Resources Research Institute under Grant A-029 IA. The technique for evaluation of α and β was developed in the course of a research programme on ice ripples sponsored by the National Science Foundation under Grant GK35918X.

REFERENCES

ANDERSON, A. G. 1953 The characteristics of sediment waves formed by flow in open channels. *Proc. 3rd Mid-Western Conf. on Fluid Mech., University of Minnesota*, pp. 379–395.

ASHIDA, K. & TANAKA, Y. 1957 A statistical study of sand waves. *Proc. 12th Congr. Int. Assn. for Hyd. Res., Ft. Collins*, vol 2, pp. 103–110.

ENGELUND, F. 1969 On the possibility of formulating a universal spectrum function for dunes. *Tech. Univ. Denmark Hydr. Lab., Progr. Rep.* no. 18, pp. 1–4.

ENGELUND, F. 1970 Instability of erodible beds. *J. Fluid Mech.* **42**, 225–244.

GRADOWCZYK, M. H. 1968 Wave propagation and boundary instability in erodible-bed channels. *J. Fluid Mech.* **33**, 93–112.

GRADOWCZYK, M. H. 1971 Interfacial instability between fluids and granular beds. *Proc. IUTAM Symp. on Instability of Continuous Systems, Herrenalb, Germany*, pp. 143–150. Springer.

HAYASHI, T. 1970 Formation of dunes and antidunes in open channels. *Proc. A.S.C.E., J. Hyd. Div.* **96**, 357–366.

HINO, M. 1968 Equilibrium-range spectra of sand waves formed by flowing water. *J. Fluid Mech.* **34**, 565–573.

JAIN, S. C. 1971 Evolution of sand wave spectra. Ph.D. thesis, Dept. of Mech. & Hyd., University of Iowa.

JAIN, S. C. & KENNEDY, J. F. 1971 The growth of sand waves. *Proc. Int. Symp. on Stochastic Hydraulics*, pp. 449–471. Pittsburgh University Press.

KENNEDY, J. F. 1963 The mechanics of dunes and antidunes in alluvial channels. *J. Fluid Mech.* **16**, 521–544.

KENNEDY, J. F. 1969 The formation of sediment ripples, dunes, and antidunes. *Ann. Rev. Fluid Mech.* **1**, 147–168.

LIGHTHILL, M. J. 1953 On the critical Froude number for turbulent flow over a smooth bottom. *Proc. Camb. Phil. Soc.* **49**, 704–706.

NORDIN, C. F. 1971 Statistical properties of dune profiles. *U.S. Geol. Survey, Prof. Paper* 562-F. U.S. Government Printing Office.

NORDIN, C. F. & ALGERT, J. H. 1966 Spectral analysis of sand waves. *Proc. A.S.C.E., J. Hyd. Div.* **92**, 95–114.

RAICHLEN, F. & KENNEDY, J. F. 1965 The growth of sediment bed forms from an initially flattened bed. *Proc. 11th Cong. Int. Assn for Hyd. Res., Leningrad*, vol. 3, paper 3.7.

REYNOLDS, A. J. 1965 Waves on the erodible bed of an open channel. *J. Fluid Mech.* **22**, 113–133.

SMITH, J. D. 1970 Stability of a sand bed subjected to a shear flow of low Froude number. *J. Geophys. Res.* **75**, 5928–5940.